IJPSR (2019), Volume 10, Issue 3 (Research Article)

INTERNATIONAL JOURNAL OF PHARMACEUTICAL SCIENCES AND RESEARCH

Received on 23 June 2018; received in revised form, 31 August 2018; accepted, 06 September 2018; published 01 March 2019

ROSMARINIC ACID LOADED CHITOSAN NANOPARTICLES FOR WOUND HEALING IN RATS

Taha Umair Wani [1], Syed Naiem Raza [* 2] and Nisar Ahmad Khan [2]

Department of Pharmaceutics [1], I.S.F. College of Pharmacy, Punjab Technical University, Moga - 142001, Punjab, India.
Department of Pharmaceutical Sciences [2], University of Kashmir, Srinagar - 190006, Jammu & Kashmir, India.

Keywords:

Chitosan Nanoparticles, Hydrogel, Rosmarinic acid, Sustained release, Wound Healing

Correspondence to Author:
Syed Naiem Raza

Assistant Professor, Department of Pharmaceutical Sciences, University of Kashmir, Srinagar - 190006, Jammu & Kashmir, India.

E-mail: syednaiem369@gmail.com

ABSTRACT: Drug release properties from dosage forms can be modified by using many rate controlling polymers. Such controlled release properties from carrier systems are desirable since efficient drug delivery is achieved. The aim of the present study was to develop efficient chitosan nanoparticles loaded with rosmarinic acid (RA) and evaluate its drug release properties and wound healing efficiency in rats. Antimicrobial activity and wound healing effect of RA is well established and reported by many workers. Chitosan is also well known for possessing rate controlling properties. For proper application over wounds, the nanoparticles were incorporated into carbopol 940 hydrogel. A fourteen-hour *in-vitro* release study was carried out to evaluate the drug release efficiency and drug release kinetics of the nanoparticles. Other parameters evaluated were particle size, polydispersity index (PDI), zeta potential, morphology. Carbopol 940 hydrogel was evaluated for optimum viscosity (18.43 ± 1.7), swelling (250 ± 7.9) and spreadability (31 ± 1.5). The *in-vivo* study was carried out in three groups of animals, those treated with gel containing RA loaded chitosan nanoparticles (RA-NP gel), gel containing only drug (RA gel), and untreated control group. Excision wound model in Wistar rats was used for the investigation of effective healing of wounds. The wound healing efficiency was evaluated by measuring the percentage of wound closure throughout 21 days. Best results were observed in the case of gel containing RA loaded chitosan nanoparticle in comparison with other animal groups.

INTRODUCTION: For proper treatment of a disease or pathological condition it is important to maintain a constant therapeutic drug concentration at the site of action. Controlled or sustained nano drug delivery systems have made it possible to maintain a constant drug concentration at the desired site.

QUICK RESPONSE CODE

DOI: 10.13040/IJPSR.0975-8232.10(3).1138-47

The article can be accessed online on www.ijpsr.com

DOI link: http://dx.doi.org/10.13040/IJPSR.0975-8232.10(3).1138-47

Nanodevices in past decades have been largely investigated for the delivery of a large number of drugs [1, 2, 3], proteins, peptides [4, 5] and genes [6], *etc*. These carriers have been used for the improvement of various physicochemical and pharmacokinetic properties of the drugs like solubility, dissolution, absorption, bioavailability, *etc*. [7]

The drugs with very low absorption have been improved to absorption by many folds using nanosystems. This has ultimately helped in increasing the bioavailability of the drugs and hence reduction in dose and thereby a low risk of toxicities [8]. So far, nanoparticles have been investigated for improving drug absorption to a

large number of organs such as lungs [9, 10], kidney [11], liver [12, 13], brain [14], eyes, skin, *etc*. which has proven efficient and beneficial. Local unloading of drugs at the site of action has been achieved by the use of novel nanocarriers. Topical delivery of drugs to skin using nanosystems has been found advantageous in maintaining a constant and uniform therapeutic drug level over the skin for many skin conditions like inflammation, bacterial or fungal infections, wounds [15, 16], *etc*.

Topical route of drug delivery is a more convenient way of approaching skin pathology like wounds than any other route, and it offers fewer side effects. The main target of the drugs used for the treatment of wounds is the bacterial load that hinders the healing process. Local delivery of drugs is always advantageous and desirable. Addressing wounds topically/locally with antibiotics may decrease the dose by many folds and lessen the toxic effects and decrease the chances of resistance to the antibiotics.

RA is a novel drug that possesses a series of actions. Among the various actions of RA antioxidant [17, 18] anti-inflammatory [19] and antimicrobial actions [20] are most prominent and extensively studied. RA has been previously investigated for antimicrobial action, and studies over the wound healing effects of RA have already been reported [21] RA has been used with other antimicrobials (Cefuroxime) to increase the effectiveness for healing the wounds [22].

Chitosan nanoparticles (CHNPs) have been largely investigated for targeted and controlled delivery of drugs to specific sites [23, 24, 25, 26]. Chitosan is the most extensively studied polymer for the preparation of nanoparticles owing to its versatile biocompatibility, biodegradability, nontoxicity, and inexpensiveness. Its hydrophilic nature and solubility profile impart nanoparticles immense capability of controlling the drug release. Carbopol 940 was used as a hydrogel system that possesses some extraordinary properties making the gel outstanding for application over skin for a condition like wounds. Among some other outstanding properties of the hydrogels is their self-healing ability wherein new bonds in them spontaneously form upon the breakage of the older bonds [27]. Because of unique properties of hydrogels to retain high amounts of water they create a moist environment over the wound that reduces the worsening of the necrotic tissue [28]. Modern research suggests that wounds heal faster in a moist environment, and the hydrogel is a perfect option [29, 30, 31]. In the presence of moisture compared to the dry wound the tissues are prevented from dehydration and hence cell death is prevented. Further, angiogenesis is hastened, fibrin and dead tissue breakdown increases and potentiate the growth of new cells by increasing the interaction of growth factors with the receptors of target cells [32]. Topical application of hydrogel gives a soothing effect by providing a soothing barrier that acts as an insulator for the wound against external hot and cold environments that is very effective in treatment for conditions like wounds [33].

In this perspective chitosan nanoparticles loaded with the therapeutic agent, RA was developed in the form of a gel using carbopol 940 and evaluated for wound healing efficiency in rats.

MATERIALS AND METHODS:

Materials: Chitosan was purchased from Sigma Aldrich; Carbopol 940, Triethanolamine and Tripolyphosphate (TPP) from Himedia. Rosmarinic acid was purchased from Sigma Aldrich. Other chemicals used were of analytical grade.

Methods:

Preparation of Nanoparticles: Chitosan nanoparticles were prepared by ionic gelation method [34, 35, 36]. 0.2% chitosan solution was prepared by adding 200 mg of chitosan to 100 ml of 2% acetic acid in small amounts since chitosan shows better solubility in acidic medium. Using a digital homogenizer, the solution was constantly stirred at 6000 rpm to obtain a homogenous solution. For cross-linking of chitosan in nanoparticles, an ionic cross-linking agent, tripolyphosphate (TPP) was used. 10 mg of RA was dissolved in 10 ml of 0.1% TPP solution prepared in distilled water which was then added dropwise to 10 ml of prepared 0.2% chitosan solution while homogenizing it at a constant speed of 6000 rpm for 10 min. Finally, the CHNPs so formed were separated from the solution by centrifugation (R-24C Remi Instruments) at 15000 rpm for 30 min and freeze-dried to get nano-particles in powder form.

Evaluation of Nanoparticles:

Particle Size, PDI and Zeta Potential: The particle size, particle size distribution and zeta potential of the prepared nanoparticles were determined by zeta size analyzer (Shimadzu, Japan) equipped with the Wing software (version 1201). The mean particle size, PDI and zeta potential of the diluted homogeneous suspensions were recorded, subsequently. Each result was recorded in triplicate. The results were then confirmed by transmission electron microscopy (TEM 906, Leo, Germany).

Entrapment Efficiency: The amount of RA entrapped in the nanoparticles was determined by UV spectrophotometry (Shimadzu UV-160 spectrophotometer, Kyoto, Japan). Each sample preparation, containing 10 mg of the drug, was centrifuged at 15000 rpm for 30 min and the supernatants analyzed for absorbances at λ_{max} 324 nm using UV spectrophotometer. Values of absorbances obtained were quantified in mg of the drugs present in the supernatant. Hence % age drug entrapment was calculated in comparison with the initial amount of the drug in the nanoparticles.

$$EE\% = \frac{\text{Total drug} - \text{Free drug}}{\text{The total drug in nanoparticles}}$$

Preparation of Nanoparticle Loaded Hydrogel: 1.2 mg of Carbopol 940 was dispersed in 50ml of distilled water. The solution was gently and constantly stirred till a homogenous gel was obtained. Dried drug-loaded nanoparticles of RA were dispersed separately in a sufficient amount of distilled water which was added to the above dispersion to form a 1.2% gel. The gel was gently homogenized for the uniform distribution of the nanoparticles in the gel. To this 2 ml of 50%, triethanolamine was added and mixed till a viscous, and clear gel was formed [37].

***In-vitro* Evaluation of Nanoparticle Loaded Gel:**

Measurement of pH: The pH of the carbopol gel was determined by a digital pH meter (Model MK–VI, Kolkata, India).

One gram of gel was dissolved in 25 ml of distilled water, and the electrode was then dipped into gel formulation for 30 min until constant reading obtained. The measurements of the pH of each formulation were replicated three times.

The degree of Swelling: The degree of swelling of the developed gel was calculated by the following equation. The test was carried out in PBS buffer pH 5.5 at 37 °C [38].

$$\text{Degree of swelling (\%)} = \frac{M_F - M_I}{M_I} \times 100$$

Where M_F (final weight) is the weight of the swollen gel sample, M_I is the initial mass of the sample immersed in a buffer medium.

Spreadability: Spreadability was determined by a wooden block and glass slide apparatus. 0.1 gm of the gel was applied to the glass slide, and about 20 g of weight was applied to the pan and the time for the upper slide to separate completely from the fixed slide was noted [39]. By applying the following formula spreadability in g.cm/sec was calculated.

$$S = M.L / T$$

Where,
S is the spreadability of the gel
M is the weight tied to the upper slide
L is the length of the glass slide
T is the time (in a sec) taken by the upper slide to completely separate from the lower one.

Rheological Measurements: The rheological measurements were performed on the Brookfield Rheometer RVDV Pro II. All measurements were carried out at room temperature 25 ± 10 °C. The rheological properties of the formulated gels were studied at three different shear rates (rpm) and the viscosity was measured in Pa.sec. 30 g gel was placed in a beaker of volume 50 mL. The speed of the spindle was increased to 400 s^{-1} and then decreased up to 0. From the data of shear rate, shear stress and viscosity different graphs were plotted. Ostwald-de Waele power-law model was used for the determination of consistency index (K) and flow index (n) according to the equation

$$\tau = KD^{\eta}$$

Where τ, is the shear stress and D is the shear rate. The slope of the graph obtained between log τ versus log D gave the flow index (n), and the antilog of the y-intercept represented the consistency index (K). An n value less than 1 ($n<1$) means that the gel is pseudoplastic while $n>1$ means the gel follows shear thickening behavior [40].

TEM Studies: Optimized drug-loaded nanoparticles were visualized under TEM for determining the shape and morphology of prepared nanoparticles. 1% solution of Phospho tungstenic acid (PTA) was prepared and coated to the Copper disc, followed by coating with the formulation. This disc was put into the disc holder, and images of nanoparticles scanned.

***In-vitro* Drug Release:** *In-vitro* drug release studies were performed for the prepared individual nanoparticles and the gel in vessels each containing 30 ml PBS buffer 5.5. The vessels were incubated in shaking incubator at 37 °C with constant orbital shaking at (100 rpm). Samples of 2 ml in triplicate at specific intervals of time were taken and replaced by the same volume of fresh PBS medium (5.5). The aliquots were analyzed for the concentration of the drug using UV spectrophotometer. The data was used for calculating the % cumulative age amount of each drug at respective intervals of time and was plotted against the time in hours.

Mechanism of Drug Release: The release pattern from the samples was evaluated by using various mathematical models. The release data were fitted to the mathematical models like zero-order (Eq. 1), first-order (Eq. 2), Peppas (Eq. 3) and Higuchi models (Eq. 4) using following equations [41].

$$(W_o - W_t) / W_o = k_t / W_o \quad \ldots\ldots \text{(Eq. 1)}$$

$$log\ C = logC_0 - \frac{k_1 t}{2.303} \quad \ldots\ldots \text{(Eq. 2)}$$

$$\frac{M_t}{M_\infty} = k_{KP} t^n \quad \ldots\ldots \text{(Eq. 3)}$$

$$f_t = Q = KH \times \sqrt{t} \quad \ldots\ldots \text{(Eq. 4)}$$

Statistical Analysis: Results are presented as Mean ± SD. The statistical analysis was evaluated using two-way ANOVA followed by Bonferroni post-test whereas two-way ANOVA followed by Tukey post-test was used for column analysis and P values ($P<0.001$ and $P<0.05$) were considered to be significant.

***In-vivo* Studies:** Male Wistar strain rats of either sex weighing 150-200 g were procured from the Central animal house, ISF College of Pharmacy, Moga, Punjab. The rats were maintained at optimum standard housing conditions and were fed with a suitable commercial diet (Hindustan Lever Ltd., Bangalore) and watered *ad libitum* during the experiment. The Institutional Animal Ethical Committee permitted the study (Reg. No. ISFCP/IAEC/CPCSEA/Meeting No 10/2014/ Protocol No. 177).

Induction of Wound: Excision wound model as described by Morton and Malone (1972) using thiopental sodium as the anesthetic was used to induce wounds in rats. Hair was removed by electric clipper. The skin of the dorsal thoracic region was excised to full thickness with the help of a surgical blade to obtain a wound area of about 200 mm^2.

Wound Healing: Three groups of six animals each were used for evaluating the wound healing effect of the formulations in excision wound models. Group I was taken as the control, group II was RA gel treated group and group III was RA-NP gel treated group. The excision wounds on the dorsal side of the rats were created as described by Morton and Malone (1972) [42], using thiopental sodium as an anesthetic.

The drugs except in case of control were applied topically daily from the first day of study until the epithelialization was complete. Wound healing was monitored by the wound closure area. The wound area measurements were done using mm^2 graph paper on the 7th, 14th and 21st days to determine the percentage of wound closure.

RESULTS AND DISCUSSION:

Evaluation of Nanoparticles:

Particle Size and PDI: RA nanoparticles of mean particle size 276.3 ± 18.45 nm and mean PDI 0.215 ± 0.02 were obtained. The amounts of chitosan and TPP used significantly influenced the particle size and PDI showing a proportional increase **Fig. 1**. Increasing the amount of drug also increased the particle size and PDI **Fig. 2**.

A drug-polymer ratio of 0.5:1 yielded nanoparticles of increased entrapment efficiency and optimum mean particle size and PDI. The size of nanoparticles was found to increase upon increasing chitosan: PP ratio. This increase in size was considered possibly due to an increased collision of the chitosan chains with TPP ions. A ratio of 5:1 of Chitosan: TPP was considered

optimum as it produced particles of optimum size range, minimum polydispersity index and also increased drug entrapment efficiency (EE).

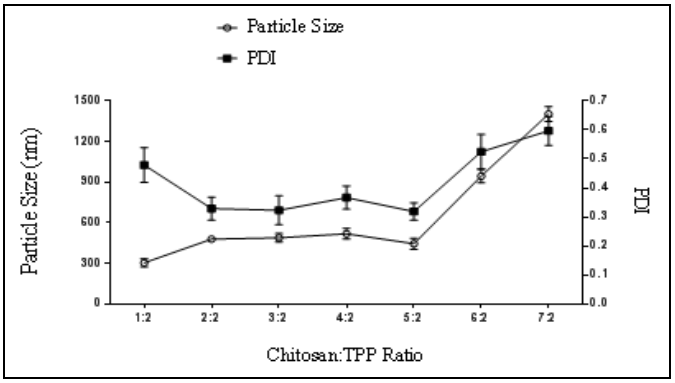

FIG. 1: EFFECT OF CHITOSAN: TPP RATIO ON PARTICLE SIZE AND PDI OF CHITOSAN NANOPARTICLES

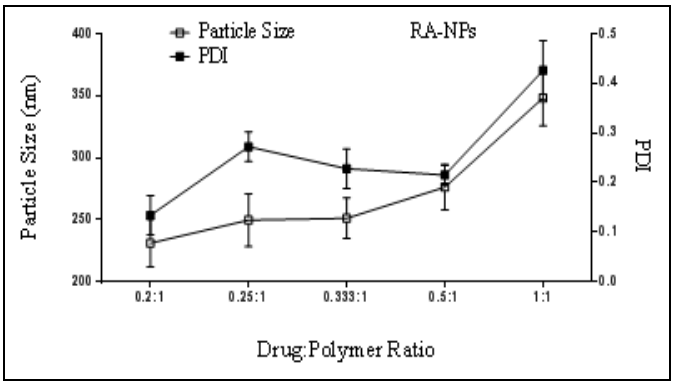

FIG. 2: EFFECT OF DRUG: POLYMER RATIO ON PARTICLE SIZE AND PDI OF CHITOSAN NANOPARTICLES

Zeta Potential: Chitosan nanoparticles are formed by the linkage of cationic ammonium (NH_3^+) groups of chitosan and anionic phosphate groups of TPP. The surface charge on chitosan nanoparticles is defined by the number of unneutralized ammonium groups in chitosan. Since the number of positively charged NH_3^+ groups of chitosan is more than a number of negatively charged phosphate groups of TPP, the net charge on the nanoparticles is positive. Zeta potential on the chitosan nanoparticles was found to be +32 ± 2. It was observed that with an increase in chitosan: TPP concentration ratio zeta potential of nanoparticles increased. This may be explained by the fact that when chitosan: TPP ratio is increased the number of molecules of chitosan also increase and hence the number of NH_3^+ groups. The increase in the number of NH_3^+ groups increases the net positive surface charge of chitosan nanoparticles.

Entrapment Efficiency: Entrapment efficiency of RA loaded nanoparticles was estimated and repeated three times. All the formulations showed good reproducible results. Entrapment efficiency of RA loaded nanoparticles was found to be 86.22 ± 2.5%. Effect of the amount of the drug used is shown in **Table 2** and **3**. The nanoparticle formulation showed an increase in entrapment efficiency with an increase in drug-polymer ratio up to 0.5:1. Beyond this ratio entrapment efficiency almost remained constant.

This may be explained by the fact that initially the nanoparticles were not saturated with the drug, the increase in the drug: polymer ratio increased the availability of the drug for encapsulation. Increase in the amount of drug entrapped in the nanoparticles eventually increased the size of the nanoparticles. With further increase in the amount of drug, no further drug loading occurred keeping the particle size constant.

TABLE 1: EFFECT OF DRUG/POLYMER RATIO ON ENTRAPMENT EFFICIENCY OF RA

Amount of Drug (g)	Drug/Polymer	EE
4	0.2:1	56.63 ± 1.3
6	0.3:1	64.14 ± 2.2
8	0.4:1	77.33 ± 1.9
10	0.5:1	86.22 ± 2.5
12	0.6:1	86.47 ± 2.3

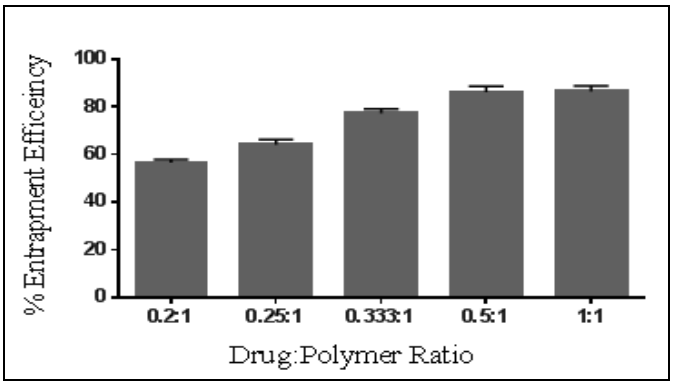

FIG. 3: EFFECT OF DRUG: POLYMER RATIO ON ENTRAPMENT EFFICIENCY OF CHITOSAN NANO-PARTICLES

TEM Studies: TEM was carried out for optimized drug-loaded nanoparticles for determining the shape and morphology of prepared nanoparticles. The TEM image of RA nanoparticles is shown in **Fig. 4**. The particle size and the surface morphology of the nanoparticles visible from the images fall in the optimum range.

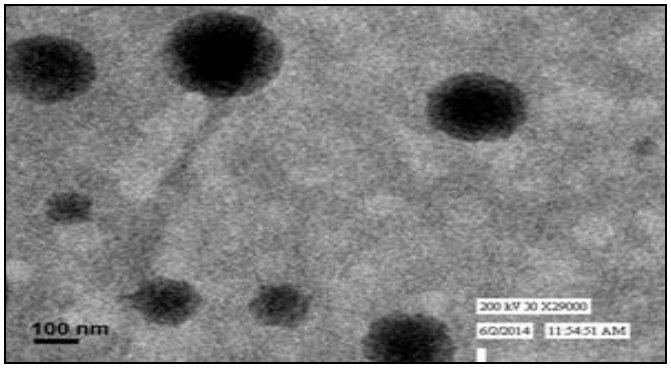

FIG. 4: TEM IMAGE OF CHITOSAN NANOPARTICLES

***In-vitro* Release:** *In-vitro* release properties of RA were studied from RA-NPs and RA-NP gel in vessels each containing PBS buffer at pH 5.5. The formulations were placed in dialysis bags with a pore size of 12000 Da and submerged in the medium.

Chitosan used in nanoparticles imparted sustained release to the drug wherein the drug was released up to greater than 85% from RA-NPs in 12 h. The release rates of the RA loaded nanoparticles were compared to the release rate from the gel containing RA nanoparticles. The employment of carbopol gel further extended the drug release to about 14 h. This was attributed to the swelling mechanism of the gel that further sustained the release of the drug from the gel. The *in-vitro* drug release from RA-NPs and drug release from RA-NP gel is demonstrated in **Fig. 5** and **Fig. 6** from which it is evident that the release of the drugs from the CHNPs was sustained throughout about 12 h and employment of hydrogel further sustained the drug release to a period of 14h.

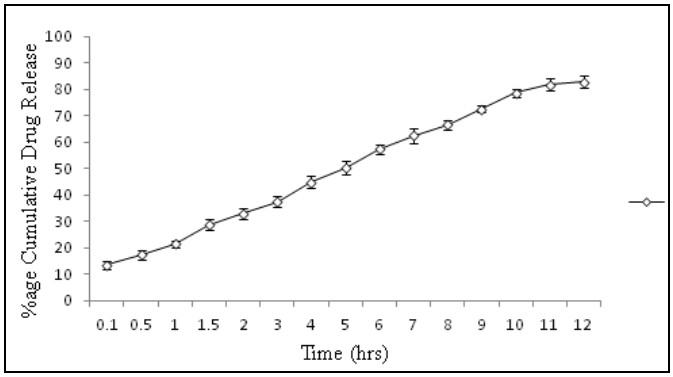

FIG. 5: % AGE CUMULATIVE DRUG RELEASE FROM RA-NPs

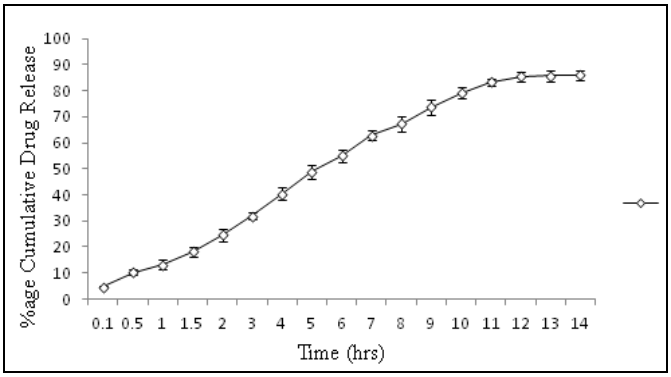

FIG. 6: % AGE CUMULATIVE DRUG RELEASE FROM RA-NP GEL

TABLE 2: *IN-VITRO* DRUG RELEASE FROM NANOPARTICLES AND GEL IN PBS AT pH 5.5

Formulation	% Age Drug Release	Time of Max Release
RA-NP	83.82 ± 2.23	12 h
RA-NP GEL	85.92 ± 1.7	14 h

Release Kinetics and Mechanism of Drug Release from Nanoparticles: To understand the kinetics of drug release from the nanoparticles different kinetic models were applied that included zero order, first order, Peppas and Higuchi models. Release model curves for RA-NPs are represented in **Fig. 7**. From the curves obtained it was observed that RA-NPs showed highest regression values for peppas curve (R^2 = 0.993).

Hence it was inferred from the curves that the drug release from the nanoparticles followed Peppas kinetics wherein the nanoparticles release the drug by erosion and diffusion mechanism hence releasing the drug in a sustained manner.

TABLE 3: R^2 VALUES OF DIFFERENT KINETIC DRUG RELEASE MODELS OF CHITOSAN NANOPARTICLES

Nanoparticle	RA-NPs
R^2 for zero-order model	0.976
R^2 for the first-order model	0.991
R^2 for Peppas model	0.993
R^2 for Higuchi model	0.946

Evaluation of the Hydrogel: The developed hydrogel was evaluated for gel concentration, pH, viscosity, swelling index, spreadability, *etc*. **Table 6**.

pH: The pH of the gel was found to decrease from 6.8 to 5.6 as the concentration of the carbopol 940 increased from 0.4 to 1.2%. This was due to the slightly acidic nature of the polymer.

The pH was adjusted by the addition of 50% triethanolamine. The pH of the final optimized 1.2% gel was found to be 5.9 ± 0.11.

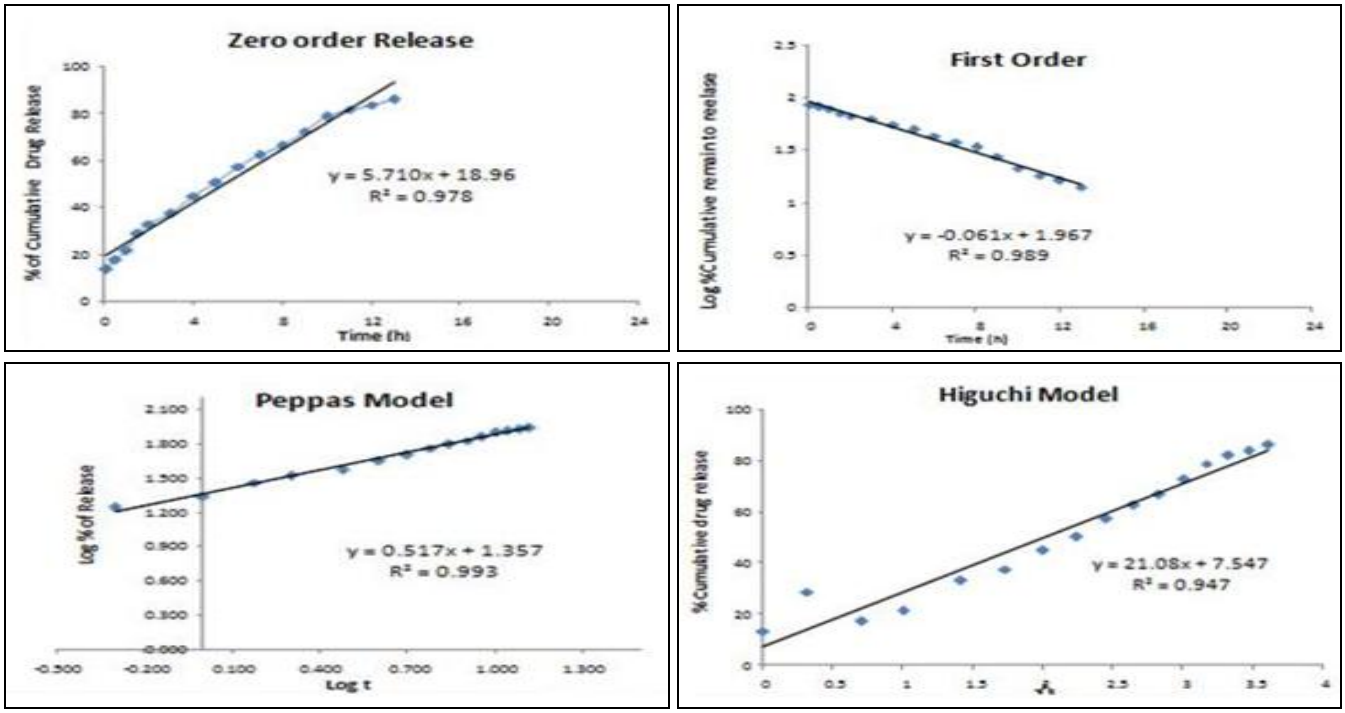

FIG. 7: KINETIC DRUG RELEASE MODELS FOR DETERMINING RATE OF DRUG RELEASE FROM RA NANOPARTICLES

Rheological Measurements: The rheological behavior of topical gel formulations was investigated since it describes spreadability and retention time of the gel formulation on the surface of the skin. The effect of different concentrations of Carbopol on viscosity was also evaluated. The viscosities of Carbopol gel containing 0.4%, 0.8%, 1.2% and 2.5% w/v Carbopol were 2.32 ± 0.15; 5.16 ± 0.9; 18.43 ± 1.7 and 25.37 ± 1.9 Pa.sec, respectively. This increase in viscosity was attributed to the increased cross-linking of the polymer network as the concentration of carbopol increased. The plot of the shear rate *vs*. the shear stress of the optimized gel formulation is shown in **Fig. 8** which shows pseudoplastic behavior of the gel wherein shear stress increases with increasing shear rate with yield value (non-Newtonian). The slope (or flow index, n) of the log plot of shear stress versus shear rate was found to be less than 1 (n = 0.572), hence confirming a pseudoplastic behavior **Table 6**. Thixotropic behavior of the gel is depicted by the viscosity versus time graph wherein the viscosity at constant shear rate decreased with time as shown in **Fig. 9**.

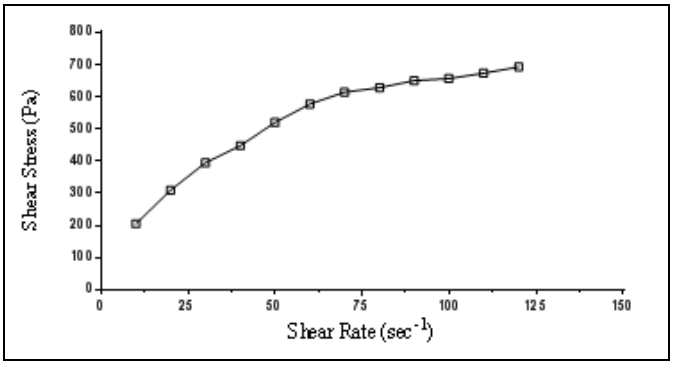

FIG. 8: RHEOLOGY OF OPTIMIZED 1.2% HYDROGEL

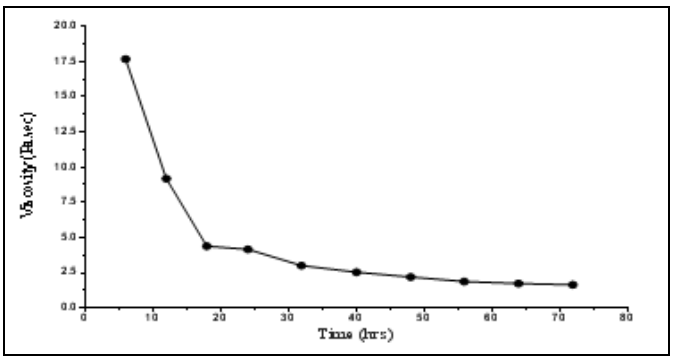

FIG. 9: VISCOSITY OF THE GEL DECREASES WITH TIME AT CONSTANT SHEAR RATE INDICATING A THIXOTROPIC BEHAVIOR OF THE GEL

Degree of Swelling: Swelling is an important parameter for the hydrogels to evaluate since the release rate of the drugs from the hydrogels depend upon their swelling properties. The swelling index of the optimized 1.2% gel was found to be 250 ± 7.9%.

Spreadability: Spreadability determines the retention properties of the hydrogel over the skin and the area of the skin that comes in contact with the drug. The spreadability of the optimized formulation was found to be 31 ± 1.5 g.cm/sec.

TABLE 4: OPTIMIZATION OF HYDROGEL

Formulation	Conc. of gel (w/v)	pH	Viscosity (Pa.sec)	% Swelling Index	Spreadability (g.cm sec^{-1})
F1	0.4 %	6.8 ± 0.18	2.32 ± 0.15	20 ± 2.4	89 ± 3.3
F2	0.8 %	6.1 ± 0.16	5.16 ± 0.9	100 ± 4.5	60 ± 2.5
F3	1.2 %	5.9 ± 0.11	18.43 ± 1.7	250 ± 7.9	31 ± 1.5
F4	2.5 %	5.6 ± 0.14	25.37 ± 1.9	450 ± 11.3	17 ± 1.9

***In-vivo* Studies:**

Wound Closure: The therapeutic efficacy of the developed formulation was evaluated using the excision wound model in Wistar rats as described by Morton and Malone (1972). Excision wound was created by excising a 2 cm^2 area to the full thickness of the skin. For evaluation of the wound healing efficacy RA gel and RA-NP gel on the animals were examined by measuring the wound area every 7^{th} day for 21 days using mm square graph paper. The healing process was found significantly faster in RA-NP gel treated group as compared to RA gel treated group. The physical examination of the wound area showed a greater amount of wound closure for RA-NP gel than RA gel and control group **Table 5**. This is further illustrated in **Fig. 10** and **Fig. 11**.

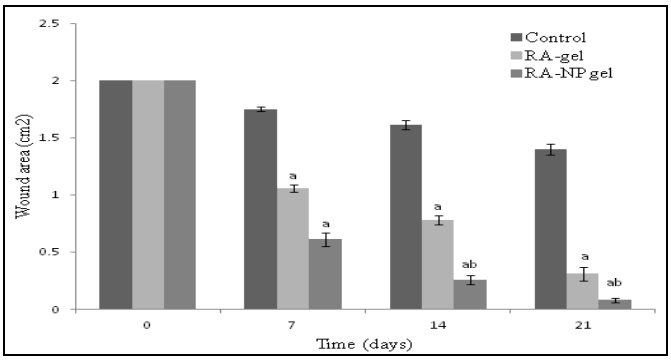

FIG. 10: EFFECT OF, RA GEL AND RA-NP GEL ON WOUND AREA. a P<0.05 VERSUS CONTROL; b P<0.05 VERSUS RA-GEL

A: Control group

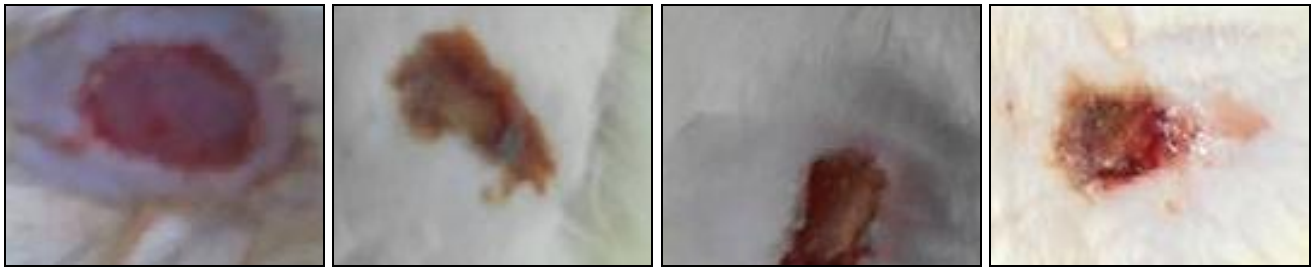

Day 0 **Day 7** **Day 14** **Day 21**

B: RA gel group

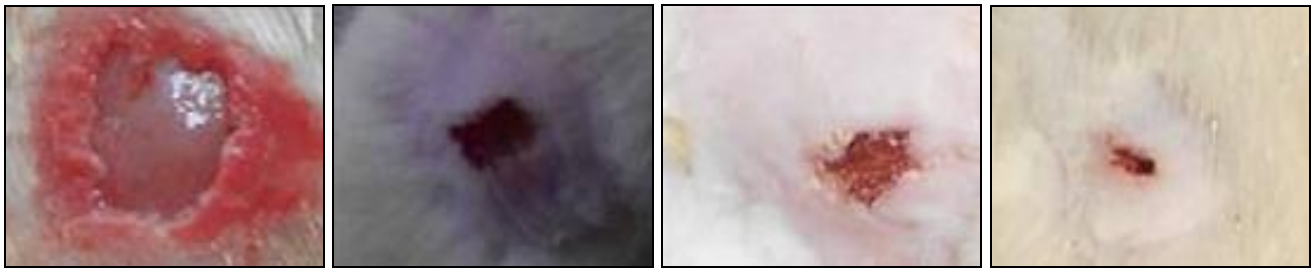

Day 0 **Day 7** **Day 14** **Day 21**

C: RA-NP gel Group

Day 0 **Day 7** **Day 14** **Day 21**

FIG. 11: PHYSICAL EXAMINATION OF WOUND AREA AT DIFFERENT INTERVALS OF TIME (IN DAYS): (A) CONTROL, (B) RA GEL TREATED, (C) RA-NP GEL TREATED

TABLE 5: WOUND CLOSURE AREAS OF CONTROL AND TREATED GROUPS

Time (in Days)	Wound area (in cm^2)		
	Control	RA gel	RA-NP gel
0	2.0 ± 0	2.0 ± 0	2.0 ± 0
7	1.75 ± 0.02	1.06 ± 0.03	0.61 ± 0.06
14	1.61 ± 0.04	0.98 ± 0.04	0.26 ± 0.04
21	1.40 ± 0.05	0.31 ± 0.06	0.08 ± 0.02

Skin Irritation Test: All the types of applied gels showed no kind of reactions on the skin. There was no sign of any erythema/eschar and edema on rat skin which indicates the compatibility of the gel with the skin.

CONCLUSION: RA loaded nanoparticles were successfully prepared by ionic gelation technique. The developed RA-NP gel formulation showed a higher degree of wound closure (faster wound healing) than the RA-gel formulation. Skin irritation studies also showed no sign of erythema/eschar or edema on rat skin which indicated the compatibility of the gel with the skin. It is therefore concluded that hydrogels containing RA loaded hydrogel are more efficacious than hydrogel containing only RA without prior loading into nanoparticles.

ACKNOWLEDGEMENT: The authors are thankful to the faculty of ISF College of Pharmacy Punjab India for providing adequate facilities to conduct this work. Also, partial support for the work was provided by the Department of Pharmaceutical Sciences, University of Kashmir India.

CONFLICT OF INTEREST: The authors declare no conflict of interest regarding the publishing of this article.

REFERENCES:

1. Couvreur P: Nanoparticles in Drug Delivery: Past, Present and Future. Advanced drug delivery reviews 2013; 65(1): 21-23.
2. Sanjeeb KS, Ranjita M and Suphiya P: Nanoparticles: A Boon to Drug Delivery, Therapeutics, Diagnostics and Imaging; Nanomedicine in Cancer 2017; 73-124.
3. Tianmeng S, Yu SZ, Bo P, Dong CH, Miaoxin Y and Younan X: Engineered Nanoparticles for drug delivery in cancer therapy; Angewandte Chemie International Edition 2014; 53(46): 12320-64.
4. Yeonhee Y, Yong WC and Kinam P: Nanoparticles for oral delivery: targeted nanoparticles with peptidic ligands for oral protein delivery; Advanced drug delivery reviews 2013; 65(6): 822-32.
5. Hong Z, Zhi YL, Lara Y, Arvind D, Xin Z and Jun W: Polymer-based nanoparticles for protein delivery: design, strategies and applications; Journal of Materials Chemistry B 2016; 4(23): 4060-71.
6. Huayu T, Jie C and Xuesi C: Nanoparticles for gene delivery. Small 2013, 9(12): 2034-44.
7. Rashid M, Wani TU, Mishra N, Sofi HS, Ashraf R and Sheikh FA: Development and characterization of drug-loaded self-solid nano-emulsified drug delivery system for treatment of diabetes. Material Science Research India 2018; 15(1): 01-11.
8. Juliette M, Raphaël B, Xavier D, Benoît T, Isabelle T and Bertrand T: Synthetic lipid nanoparticles targeting steroid organs. Jou of Nuclear Medicine 2013, 54(11): 1996-2003.
9. Xiaoli C, Yanan L, Weiying Z, Dan D and Yuehe L: pH-sensitive zno quantum dots–doxorubicin nanoparticles for lung cancer targeted drug delivery. ACS applied materials & interfaces 2016; 8(34): 22442-50.
10. Piyush KS, Deepak KM, Nivrati J, Vaibhav R and Ashish KJ: Mannosylated solid lipid nanoparticles for lung-targeted delivery of paclitaxel. Drug development and industrial pharmacy 2015, 41(4): 640-49.
11. Chung HJC, Jonathan EZ, Paul W and Mark ED: Targeting kidney mesangium by nanoparticles of defined size. Proceedings of the National Academy of Sciences 2011; 201103573.
12. Xiaodan W, Xiangqin G, Huimin W, Yujiao S, Haiyang W and Shirui M: Synthesis, characterization and liver targeting evaluation of self-assembled hyaluronic acid nanoparticles functionalized with glycyrrhetinic acid. European Journal of Pharmaceutical Sciences 2017; 96: 255-62.
13. Dunwan Z, Wei T, Hongling Z, Gan L, Teng W, Linhua Z, Xiaowei Z and Lin M: Docetaxel (Dtx)-Loaded Polydopamine-Modified Tpgs-Pla Nanoparticles as a targeted drug delivery system for the treatment of liver cancer. Acta biomaterialia 2016; 30: 144-54.
14. Omidreza J, Shadab M, Mushir A, Sanjula B, Sahni JK, Bhavna K, Aseem B and Javed A: Design, characterization, and evaluation of intranasal delivery of ropinirole-loaded mucoadhesive nanoparticles for brain targeting. Drug development and industrial pharmacy 2015; 41(10): 1674-81.
15. Melissa P and Francois B: Nanoparticles for skin wound healing. Nano LIFE 2013; 3(3): 1342004.
16. Chiara R, Letizia F, Ilaria T, Marco R, Ivan M, Chiara G, Warren RLC, Vincenzo V, Bruno A and Carlo B: Active silver nanoparticles for wound healing. International journal of molecular sciences 2013; 14(3): 4817-40.
17. Amma GAB, Sue LFC, Margaret P and Jeffrey RF: Antioxidant activity of rosmarinic acid and its principal metabolites in chemical and cellular systems: Importance of Physico-Chemical Characteristics. Toxicology *in-vitro* 2017; 40: 248-55.
18. Marisa N, Paula P, Rute FV, Catarina PR, Amilcar R and Patrícia R: Antioxidant activity and rosmarinic acid content of ultrasound-assisted ethanolic extracts of medicinal plants. Measurement 2016; 89: 328-32.
19. Joao R, Maria EF, Andreia B, Adelaide F, Dora B, Rosario B, Catarina MMD, Ana TS, Rui P and Marisa F: Anti-inflammatory effect of rosmarinic acid and an extract of *Rosmarinus officinalis* in rat models of local and

systemic inflammation; Basic & clinical pharmacology & toxicology 2015; 116(5): 398-413.
20. Daniela B, Daniela H, Ilioara O, Brindusa T, Neli KO, Oana R, Cristina B, Radu SD and Laurian V: Assessment of rosmarinic acid content in six lamiaceae species extracts and their antioxidant and antimicrobial potential. Pak J Pharm Sci 2015; 28(6): 2297-303.
21. Yilanci S, Bali YY, Yuzbasioglu M, Unlu RE, Orhan E, Simon A, Tóth G, Demirezer LO and Kuruuzum UA: The evaluation of wound healing potential of rosmarinic acid isolated from *Arnebia purpure*. Planta Medica 2015; 81(16): PM_135.
22. Naser J, Awni AH and Kamel A: Antibacterial activity of *Rosmarinus officinalis* L. alone and in combination with cefuroxime against methicillin-resistant *Staphylococcus aureus*. Asian Pacific Journal of Tropical Medicine 2010; 3(2): 121-23.
23. Tarek AA and Bader MA: Preparation, Characterization, and potential application of chitosan, chitosan derivatives, and chitosan metal nanoparticles in pharmaceutical drug delivery. Drug design, development and therapy 2016; 10: 483.
24. Jijin G, Karam AB and Emmanuel AH: Development of antibody-modified chitosan nanoparticles for the targeted delivery of siRNA across the blood-brain barrier as a strategy for inhibiting HIV replication in astrocytes. Drug delivery and translational research 2017; 7(4): 497-506.
25. Walter ER, Adriana P, Abuzar A, Michelle AL and Tejraj MA: Targeted delivery of small interfering RNA to colon cancer cells using chitosan and pegylated chitosan nanoparticles. Carbohydrate polymers 2016; 147: 323-32.
26. Fengqiang W, Yan W, Qingzhu M, Yuan C and Bo Y: Development and characterization of folic acid-conjugated chitosan nanoparticles for targeted and controlled delivery of gemcitabine lung cancer therapeutics. Artificial cells, Nanomedicine, and Biotechnology 2017; 45(8): 1530-38.
27. German VK, Solomon FD, Victor VY and Anna CB: Towards self-healing organic nanogels: a computational approach. Nanotechnologies for the Life Sciences 2011; 10: 1-26.
28. Wani TU, Rashid M, Kumar M, Chaudhary S, Kumar P and Mishra N: Targeting aspects of nanogels: an overview. International Journal of Pharmaceutical Sciences and Nanotechnology 2014; 7(4): 2612-30.
29. Charles KF and Morris DK: Overview of wound healing in a moist environment. The American journal of surgery 1994; 167(1): S2-S6.
30. Iwona G and Helena J: Synthetic polymer hydrogels for biomedical applications. Chemistry and Chemical Technology 2010; 4(4): 297-304.
31. Karen O, Cutting KF, Alan AR and Rippon MG: The importance of hydration in wound healing: reinvigorating the clinical perspective. Journal of wound care 2016; 25(3): 122-30.
32. Catanzano O, D'esposito V, Acierno S, Ambrosio MR, Caro CD, Avagliano C, Russo P, Russo R, Miro A and Ungaro F: Alginate–hyaluronan composite hydrogels accelerate wound healing process. Carbohydrate polymers 2015; 131: 407-14.
33. Annapoorna M, Kumar PTS, Biswas R, Lakshmanan VK and Rangasamy J: Exploration of alginate hydrogel/nano zinc oxide composite bandages for infected wounds. International Journal of Nanomedicine 2015; 10(1): 53.
34. Loïc B and Catherine L: Interests of chitosan nanoparticles ionically cross-linked with tripolyphosphate for biomedical applications. Progress in polymer science 2016; 60: 1-17.
35. Neves ALP, Camila CM, Leidiani M, Humberto GR, Nivaldo CK and Hellen KS: Factorial design as tool in chitosan nanoparticles development by ionic gelation technique; colloids and Surfaces A: Physicochemical and Engineering Aspects 2014; 445: 34-39.
36. Thandapani G, Sudha PN, Florence JAK, Jayachandran V and Sukumaran A: Fabrication of letrozole formulation using chitosan nanoparticles through ionic gelation method. International Journal of Biological Macromolecules 2017; 104: 1820-32.
37. Kesavan B, Chinnala KM, Meka L, Somagoni JM, Vobalaboina V, Yamsani MMR, Jayaraman A and Velayudam R: Development of Sln and Nlc enriched hydrogels for transdermal delivery of nitrendipine: *in-vitro* and *in-vivo* characteristics. Drug development and industrial pharmacy 2009; 35 (1): 98-113.
38. Joao M, Lino F, Rui C, Manuel AR and Maria HG: Synthesis and characterization of new injectable and degradable dextran-based hydrogels. Polymer 2005; 46(23): 9604-14.
39. Gupta G and Gaud R: Release rate of nimesulide from different gallants. Indian Journal of Pharmaceutical Sciences 1999; 61(4): 227-230.
40. Mandala IG and Bayas E: Xanthan effect on swelling, solubility and viscosity of wheat starch dispersions. Food Hydrocolloids 2004; 18(2): 191-201.
41. Syed NR and Nisar AK: Role of mathematical modeling in controlled release drug delivery. Int Journal of Medical Research and Pharmaceutical Sciences 2017; 4(5): 84-95.
42. Sunil K, Subash S and Sanjay KS: An experimental evaluation on wound healing property of shigru patra ghanasatva (leaf water extract of *Moringa oleifera* Lam); Journal of Ayurveda Physicians & Surgeons (JAPS) 2017; 3(3): 57-61.

How to cite this article:
Wani TU, Raza SN and Khan NA: Rosmarinic acid loaded chitosan nanoparticles for wound healing in rats. Int J Pharm Sci & Res 2019; 10(3): 1138-47. doi: 10.13040/IJPSR.0975-8232.10(3).1138-47.